

Recent results from Double Chooz

H. WATANABE(*) for the DOUBLE CHOOZ COLLABORATION

Max-Planck-Institut für Kernphysik - Saupfercheckweg 1, 69117 Heidelberg, Germany

ricevuto il 20 Giugno 2013; approvato l'1 Luglio 2013

Summary. — Double Chooz is a reactor neutrino experiment that aims at a precise measurement of the neutrino mixing angle θ_{13} . This experiment has been detecting electron antineutrinos using a single detector, that is located ~ 1.050 m away from two reactor cores at the Chooz nuclear power station in France. This article gives a review of the θ_{13} analysis results with neutrons originated from inverse β -decay captured on gadolinium, as well as recently-reported first measurement with those on hydrogen. These results are, respectively, $\sin^2 2\theta_{13} = 0.109 \pm 0.030(\text{stat.}) \pm 0.025(\text{syst.})$ and $\sin^2 2\theta_{13} = 0.097 \pm 0.034(\text{stat.}) \pm 0.034(\text{syst.})$ obtained as best fit values to the neutrino rate and the energy spectrum. The two independent approaches demonstrate the consistency of results for θ_{13} in datasets that are statistically different and also some distinct in systematic uncertainties. Physics studies other than the θ_{13} measurement have been performed to make a direct background detection during two reactors off period, and a first test of Lorentz violation using reactor neutrinos.

PACS 14.60.Pq – Neutrino mass and mixing.

PACS 14.60.St – Non-standard-model neutrinos, right-handed neutrinos, etc..

1. – Introduction

The Double Chooz experiment is designed to make a precise measurement of the neutrino mixing parameter θ_{13} with $\bar{\nu}_e$'s from two nuclear reactors in Chooz, France. This article reports the achievements for measurement of θ_{13} using gadolinium as a standard analysis method [1], as well as the one with recently-conducted independent analysis using hydrogen [2]. Section 2 gives a brief description of neutrino oscillation. Section 3 describes the motivation, experimental site and technique, and detector concept of the Double Chooz Experiment. Section 4 briefs the prediction of number of reactor neutrinos. The detector performance via calibration is given in sect. 5. Analysis and results of θ_{13} measurement with gadolinium and hydrogen are described in sect. 6. Other physics results are introduced briefly in sect. 7 that are the direct measurement of backgrounds during the period of two reactors off [3], and a first test of Lorentz violation with reactor $\bar{\nu}_e$'s [4]. Concluding remarks and outlook are presented in sect. 8.

(*) E-mail: hideki.watanabe@mpi-hd.mpg.de

2. – Neutrino oscillation

It is well known that neutrinos change the flavours during their propagation. This has been observed by solar [5,6], atmospheric [7,8], reactor [9] and accelerator-based neutrino experiments [10-12]. Neutrino oscillations occur as a result of the non-zero neutrino mass, and the flavour eigenstates described by the mixing of the mass eigenstates [13,14]. In the framework of three neutrinos, the neutrino oscillation probability is composed of three mixing angles (θ_{12} , θ_{23} , θ_{13}), two squared mass differences (Δm_{21}^2 , Δm_{31}^2) and the CP-violation phase in lepton sector (δ_{CP}). While θ_{12} and θ_{23} have been observed by different experiments, θ_{13} was the only unknown mixing angle until recently. The first indications of its non-zero value were given by the accelerator-based experiments [15,16]. Then, it was finally observed by the short baseline (~ 1 km) reactor neutrino experiments [17-19]. In the short baseline reactor experiments, the survival probability of electron antineutrinos is described by the simple 2 flavour formalism as follows:

$$(1) \quad P(\bar{\nu}_e \rightarrow \bar{\nu}_e) \approx 1 - \sin^2 2\theta_{13} \sin^2 \frac{1.27 \Delta m_{31}^2 [\text{eV}^2] L [\text{m}]}{E [\text{MeV}]},$$

where L is the distance from the reactor cores to the detector, and E is the neutrino energy. These experiments are advantageous for the clean θ_{13} measurement since the matter effect is negligible, the survival probability is simply a function of θ_{13} and Δm_{31}^2 , and independent of δ_{CP} . The value of θ_{13} is obtained by the amplitude of oscillation *i.e.*, the energy dependent deficit of the observed number of neutrinos. Non-zero θ_{13} opens up a possibility of measuring δ_{CP} with accelerator-based experiments.

3. – The Double Chooz experiment

The Double Chooz experiment adopts two identical detectors at different baselines so that the systematic uncertainties are cancelled out. One of the two detectors is called Far Detector which is located ~ 1.050 m away from the two reactor cores under 300 m.w.e. overburden. This detector is used to see the deficit of neutrinos at the first maximum of oscillation. The other is Near Detector to be constructed at 410 m from the cores under 120 m.w.e. overburden for observing the unoscillated neutrino spectrum. At the time of writing this article, all results are obtained only with Far Detector.

The four cylindrical layer liquid structure is adopted as a detector design in Double Chooz in order to optimize the reduction of backgrounds as well as the systematic uncertainties on the $\bar{\nu}_e$ spectrum measurement. Figure 1 describes a cross-sectional view of the detector. The 10.3 m^3 gadolinium-loaded liquid scintillator is installed in the innermost part of the detector that is called Neutrino Target (NT). The whole NT with 1 g/l gadolinium is used as a fiducial volume surrounded by a 8 mm thick transparent acrylic vessel. This region is essential to identify $\bar{\nu}_e$'s through gammas with their total energy of $\sim 8 \text{ MeV}$ released from thermal neutron capture on gadolinium: neutrons are originated from inverse β -decay. NT is advantageous since the systematic uncertainties related to the event reconstruction in space can be suppressed thanks to the usage of its entire volume. The Gamma-Catcher (GC) is built for the energy recovery of escaping γ 's of annihilation or following neutron capture on gadolinium, from NT. This is a 50 cm thick layer whose volume is 22.3 m^3 filled with gadolinium-unloaded liquid scintillator in the 12 mm thick acrylic vessel. The region called Buffer functions as a shield of natural radioactivities. These are originated from photomultipliers (PMTs) mounted on its

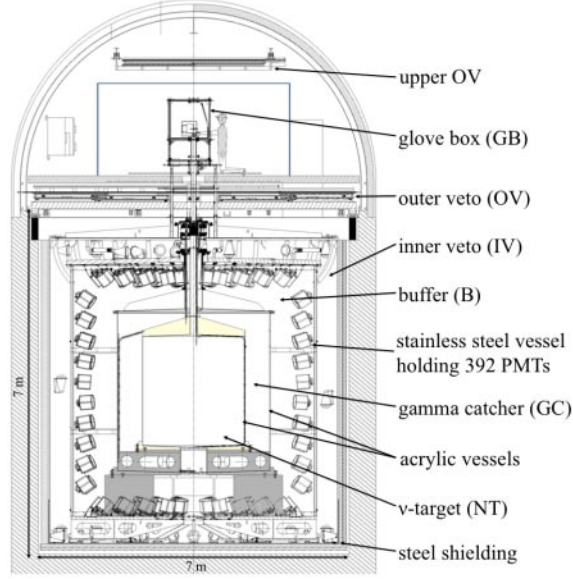


Fig. 1. – A Cross-sectional View of the Double Chooz Detector

inner walls, and from the surrounding rock. The Buffer surrounding GC is composed of the steel vessel with 110 m^3 non-scintillating mineral oil with 390 10 inch diameter Hamamatsu R7081 PMTs. These three sub-volumes consist of the Inner Detector (ID). Energy and timing information of events are collected by PMTs from the scintillation light. Inner Veto surrounds ID to veto cosmic-ray muons as well as fast neutrons to be backgrounds in ID. 78 8 inch diameter Hamamatsu R1408 PMTs are equipped on its inner walls, and 90 m^3 LAB based-liquid scintillator is filled in this region whose thickness is 50 cm enclosed by the steel vessel. Both ID and IV are surrounded by 15 cm thick steel shielding. The Outer Veto (OV) is established by the multi-layers of plastic scintillator strips above IV to cover its entire plane that enhances the power of vetoing cosmic-ray muons. The glove box is prepared at the top of the detector to guide the radioactive sources and light sources into the detector for the detector calibration. This system avoids the contamination from outside of the detector.

4. – Predicted number of reactor neutrinos

Electron antineutrinos are emitted from the decays of the fission products of ^{235}U , ^{238}U , ^{239}Pu , and ^{241}Pu at the two reactor cores in Chooz. The number of $\bar{\nu}_e$'s with no oscillation is then expected to be

$$(2) \quad N_{\nu}^{exp}(E, t) = \frac{N_p \varepsilon}{4\pi L^2} \cdot \frac{P_{th}(t)}{\langle E_f \rangle} \cdot \langle \sigma_f \rangle,$$

where N_p is the number of free protons in the detector, ε is the detection efficiency, $P_{th}(t)$ is the thermal power, and L is the baseline. $\langle E_f \rangle(t) = \sum_k \alpha_k(t) \langle E_f \rangle_k$ is the mean energy per fission of each nuclide with its fractional fission rate α_k ($k = ^{235}\text{U}, ^{238}\text{U}, ^{239}\text{Pu}$,

and ^{241}Pu) evaluated by the two complementary simulation packages DRAGON [20] and MURE [21]. The mean cross-section per fission $\langle\sigma_f\rangle$ is described as

$$(3) \quad \langle\sigma_f\rangle = \langle\sigma_f\rangle^{\text{Bugey}} + \sum_k (\alpha_k^{\text{DC}}(t) - \alpha_k^{\text{Bugey}}(t)) \langle\sigma_f\rangle_k,$$

where $\langle\sigma_f\rangle_k$ is the mean cross-section per fission isotope k and given by $\langle\sigma_f\rangle_k = \int_0^\infty dE \cdot S_k(E) \cdot \sigma_{IBD}(E)$ with $S_k(E)$ as the reference spectrum [22,23] and $\sigma_{IBD}(E)$ as the cross-section of inverse β -decay [24]. In Double Chooz, the measurement of the Bugey4 experiment [25] held at $L = 15\text{ m}$ was used as an anchor point for normalization. The second term in eq. (3) makes a correction for the difference between each of the Chooz reactor cores and Bugey4 with respect to the fuel composition. Since $(\alpha_k^{\text{DC}}(t) - \alpha_k^{\text{Bugey}}(t))$ is small, the dependence on the predicted $\langle\sigma_f\rangle$ is suppressed. The usage of Bugey4 is advantageous not only for the high accuracy of its anchoring point as 1.4% but for the minimization of the sensitivity to the effect of heavy sterile neutrinos *i.e.*, $\Delta m^2 \sim 1\text{ eV}^2$ at shorter baselines [26]. In total, the uncertainties regarding the antineutrino prediction are evaluated to be 1.76%.

5. – Detector calibration

A series of detector calibrations are conducted in Double Chooz to understand the detector performance. The radioactive source deployment systems are prepared in NT and GC with ^{60}Co , ^{68}Ge , ^{137}Cs and ^{252}Cf . These provide the energy scale determination and the reduction of its systematics, as well as the estimation of neutron detection efficiency. The embedded LED injection system is used to calibrate the PMT and electronics gain non-linearity, and also monitor the stability. Stability is also studied with cosmic-ray muon-induced spallation neutrons. The corrections of position dependence and time variation are performed by using spallation neutrons that are thermalized and then captured either on gadolinium or on hydrogen. The stability is found out to be within 1% and there is no degradation of liquid scintillator observed since the start of data-taking.

6. – θ_{13} analysis

6.1. Analysis with neutron capture on gadolinium. – The data used in the analysis here were collected between April 2011 and March 2012, and the following selection criteria were introduced to select the candidates from inverse β -decay among samples above 0.5 MeV: I) prompt events: $0.7\text{ MeV} < E < 12.2\text{ MeV}$; II) delayed events: $6.0\text{ MeV} < E < 12.0\text{ MeV}$; III) time correlation between prompt and delayed events: $2 < \Delta t < 100\ \mu\text{s}$; IV) multiplicity rejection: No valid triggers within $100\ \mu\text{s}$ prior to the prompt event, and one valid trigger within $400\ \mu\text{s}$ following this; V) further cosmogenic background rejection: Events $> 500\text{ ms}$ after a muon event with energy $> 600\text{ MeV}$; VI) μ and Fast neutron rejection: Veto prompt events in coincidence with triggers issued by OV. Events with spontaneous light emissions from PMT bases are also rejected by requesting the homogenous PMT hit pattern and small spread of pulse start time. As well, the time condition between the prompt signal and its last muon is adopted that is larger than 1 ms to reduce muon backgrounds. After the application of the selection criteria above, 8249 $\bar{\nu}_e$ candidates are remained in 227.93 livedays with 100% trigger efficiency above 0.7 MeV.

TABLE I. – *Summary of statistic and systematic normalization uncertainties relative to the total signals in gadolinium (middle) and hydrogen (right) analysis.*

Source	Uncertainty in gadolinium analysis [%]	Uncertainty in hydrogen analysis [%]
Reactor flux	1.7	1.8
Statistics	1.1	1.1
Accidentals	< 0.1	0.2
Cosmogenic ${}^9\text{Li}$	1.4	1.6
Fast neutrons (and stopping muons in Gd)	0.5	0.6
Correlated light noises	N.A.	0.1
Energy scale	0.3	0.3
Detection efficiency	1.0	1.6
Total	2.7	3.1

Remaining background events are classified into three types: accidental coincidence backgrounds, those from long-lived cosmogenic isotopes, and correlated backgrounds by fast neutrons and stopping muons.

The accidentals are caused by natural radioactivities as prompt, and neutron-like candidate as delayed. The measurement was achieved by the off-time window sampling scheme leading to the high statistical observation with spectrum. The rate of these backgrounds was evaluated to be 0.261 ± 0.002 events/day.

Cosmogenic isotopes *i.e.*, ${}^9\text{Li}$ and ${}^8\text{He}$ are produced by the muon spallation with carbon nuclei. These isotopes mimic inverse β -decay since they emit both β and neutron satisfying the delayed coincidence scheme. Also, the long lifetime of these isotopes gives a difficulty for their complete vetoing. The rate was measured from the spatial and time correlations with the parent muons by fitting the time difference. This was evaluated to be 1.25 ± 0.54 events/day.

Fast neutrons and stopping muons also mimic inverse β -decay. The former backgrounds are caused by recoiling protons as prompt and thermalized neutron capture on gadolinium as delayed. The latter backgrounds are induced by muons without triggering vetos and the following Michel electrons playing as prompt and delayed, respectively. The measurement of their rate was conducted using a higher energy window *i.e.*, $12\text{ MeV} < E < 30\text{ MeV}$ where $\bar{\nu}_e$'s are not expected. This evaluation is extrapolated down to the $\bar{\nu}_e$ selection region and the rate is found to be 0.67 ± 0.20 events/day.

The rate and shape oscillation analysis is performed by introducing 36 variable-sized binnings for the prompt energy spectrum that are composed of first and second 18 bins. The first 18 bins are given during the period of both of two reactors on, while the second 18 bins are for the period with the thermal power of either reactor less than 20%. This treatment helps better constrain of backgrounds in the fit due to the different signal to background ratio by different reactor power. χ^2 minimization approach with covariance matrix and pull terms is adopted to find the best fit oscillation parameters. Statistical and part of the systematic uncertainties are incorporated into the covariance matrix, while uncertainties are propagated into the pull terms from background rates of cosmogenic isotopes, fast neutrons and stopping muons, and energy scale as well as the Δm_{31}^2 constrained by the value in [11]. The middle column of table I shows a summary of systematic normalization uncertainties relative to the total signals. The best fit value was

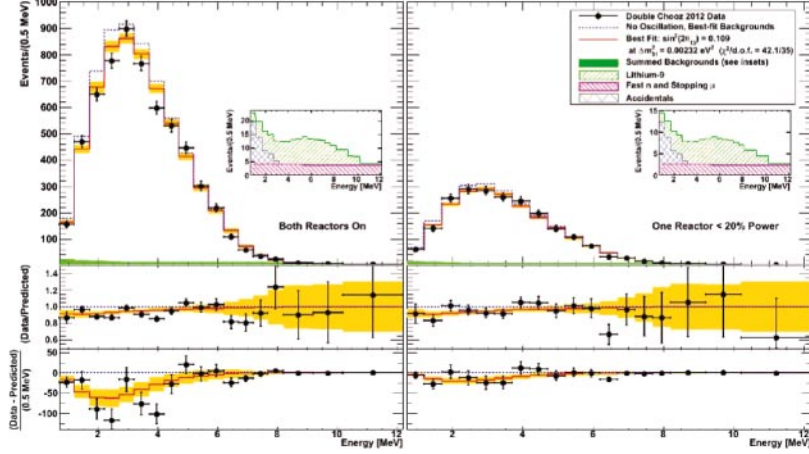


Fig. 2. – Prompt energy spectrum with observation, no oscillation prediction and the best fit with oscillation in gadolinium analysis. Left and right panels are, respectively, the spectrum during the two reactors on and either reactor’s thermal power less than 20%.

found at $\sin^2 2\theta_{13} = 0.109 \pm 0.030(\text{stat.}) \pm 0.025(\text{syst.})$ with $\chi^2/\text{n.d.f.} = 42.1/35$. Figure 2 displays prompt energy spectrum of data and the best fit case for the two different period of reactor powers. No oscillation hypothesis is excluded at 99.8% C.L. (2.9σ).

6.2. θ_{13} Analysis with neutron capture on hydrogen. – The time period of used data in this hydrogen analysis is the same as in the gadolinium analysis. $\bar{\nu}_e$ candidates are searched both at NT and GC with 2.2 MeV gammas as delayed from neutrons captured on hydrogen. Different selection criteria are adopted as follows: I) prompt events: $0.7 \text{ MeV} < E < 12.2 \text{ MeV}$; II) delayed events: $1.5 \text{ MeV} < E < 3.0 \text{ MeV}$; III) time correlation between prompt and delayed events: $10 < \Delta t < 600 \mu\text{s}$; IV) spatial correlation between prompt and delayed events: $\Delta r < 900 \text{ mm}$; V) multiplicity rejection: No valid triggers within $600 \mu\text{s}$ prior to the prompt event, and one valid trigger within $1000 \mu\text{s}$ following this. As in the gadolinium analysis, spontaneous light emissions from PMT bases are rejected, and the muon background reduction is also performed. 36284 $\bar{\nu}_e$ candidates were obtained in 240.06 livedays.

Four types of backgrounds are remained. The accidental rate is measured by 125 consecutive off-time window sampling between 1 and 1.2 s. This is evaluated to be 73.45 ± 0.16 events/day. Cosmogenic isotopes rate is estimated by fitting exponentially the time difference between the last muon and the prompt event with the lifetime of ${}^9\text{Li}$ and the constant term. This results in 2.84 ± 1.15 events/day. Fast neutron rates are estimated from their spectrum tagged by ID and IV correlation of pulse timing above 12 MeV, and result in 2.50 ± 0.47 events/day in the relevant energy region. Small contribution of spontaneous light emissions from PMT bases are also observed as correlated backgrounds producing two consecutive triggers. Measurement with volume cut on reconstructed vertex is performed to evaluate this rate as 0.32 ± 0.07 events/day.

The rate and shape oscillation analysis is conducted that is identical to the procedure in the gadolinium analysis. However, 31 variable-sized binning was prepared, instead, and only one single period is used. Incorporated systematic uncertainties are summarized in the right column in table I. As the best fit value, $\sin^2 2\theta_{13} = 0.097 \pm 0.034(\text{stat.}) \pm 0.034(\text{syst.})$ with $\chi^2/\text{n.d.f.} = 38.9/30$ is obtained as shown in fig. 3, and the consistency of

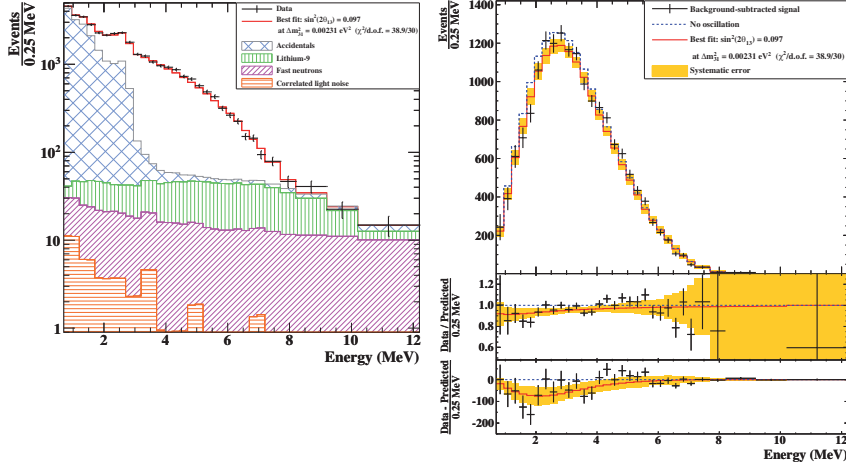


Fig. 3. – Prompt energy spectrum with $\bar{\nu}_e$ candidates and backgrounds (left); prompt energy spectrum with observation, no oscillation prediction and the best fit with oscillation (right) in hydrogen analysis.

θ_{13} from two independent approaches is confirmed. No oscillation hypothesis is excluded at 97.4% C.L. (2.0σ). Moreover, results are also consistent with those from other reactor-based and accelerator-based neutrino experiments. This is the first-ever achievement of θ_{13} measurement using hydrogen.

7. – Other physics results

Double Chooz is unique among other reactor neutrino experiments in that physics studies other than the θ_{13} measurement have been performed. Thanks to the both two reactors off for 7.53 days, a direct background observation in the oscillation analysis is conducted by using the same event selection criteria as in θ_{13} gadolinium analysis. Two selection cases are studied *i.e.*, those with or without both criteria of cosmogenic background rejection, and μ and fast neutron rejection. These are described as V) and VI) among the selection criteria in sect. 6.1. 2.7 ± 0.6 events/day without these criteria, and 1.0 ± 0.4 events/day with these are obtained. These results are consistent with their estimations *i.e.*, 3.4 ± 0.6 events/day and 2.0 ± 0.6 events/day, respectively. This study demonstrates a reliability of the background understanding in the oscillation analysis.

A first test of Lorentz violation using neutrinos from each reactor core was fulfilled. This is a search for sidereal modulation with the same dataset used for gadolinium analysis. Reactor neutrino disappearance experiment is suitable for accessing its e - τ channel. After the analysis, there are no decisive events observed and results are consistent with the sidereal time-independent neutrino oscillation. Then, the first stringent limits are placed on 14 coefficients for e - τ channel, and also limits are set on 2 coefficients for e - μ channel in the Standard Model Extension.

8. – Summary and outlook

Double Chooz has made a measurement of reactor neutrino disappearance using the events of thermal neutrons captured on gadolinium. This concludes $\sin^2 2\theta_{13} = 0.109 \pm 0.030(\text{stat.}) \pm 0.025(\text{syst.})$. The energy spectral information is incorporated in

the analysis which is unique among other reactor neutrino experiments. Furthermore, the first measurement of θ_{13} was achieved recently with thermal neutrons captured on hydrogen. This is beneficial as an independent analysis for the cross-check of the gadolinium analysis since these are statistically different and also some distinct in systematic uncertainties. $\sin^2 2\theta_{13} = 0.097 \pm 0.034(\text{stat.}) \pm 0.034(\text{syst.})$ is obtained and this confirms a consistency of the results from the gadolinium analysis. A direct background measurement for 7.53 days during two reactors off period, and a first test of Lorentz violation using reactor neutrinos have been performed as other unique researches in Double Chooz. In the future, both gadolinium and hydrogen analysis are considered to be combined that prospects the results with larger statistics and improved systematic uncertainties. Furthermore, the reduction of systematics is expected with data-taking using both Near and Far detectors that will lead to the improvement of the precision, and the robustness of θ_{13} .

REFERENCES

- [1] ABE Y. *et al.*, *Phys. Rev. D*, **86** (2012) 052008, doi:10.1103/PhysRevD.86.052008.
- [2] ABE Y. *et al.*, *Phys. Lett. B*, **723** (2013) 66, doi:10.1016/j.physletb.2013.04.050.
- [3] ABE Y. *et al.*, *Phys. Rev. D*, **87** (2013) 011102, doi:10.1103/PhysRevD.87.011102.
- [4] ABE Y. *et al.*, *Phys. Rev. D*, **86** (2012) 112009, doi:10.1103/PhysRevD.86.112009.
- [5] AHARMIM B. *et al.*, *Phys. Rev. C*, **88** (2013) 025501, doi:10.1103/PhysRevC.88.025501.
- [6] ABE K. *et al.*, *Phys. Rev. D*, **83** (2011) 052010, doi:10.1103/PhysRevD.83.052010.
- [7] ADAMSON P. *et al.*, *Phys. Rev. D*, **86** (2012) 052007, doi:10.1103/PhysRevD.86.052007.
- [8] WENDELL R. *et al.*, *Phys. Rev. D*, **81** (2010) 092004, doi:10.1103/PhysRevD.81.092004.
- [9] GANDO A. *et al.*, *Phys. Rev. D*, **83** (2010) 052002, doi:10.1103/PhysRevD.83.052002.
- [10] AHN M. H. *et al.*, *Phys. Rev. Lett.*, **90** (2003) 041801, doi:10.1103/PhysRevLett.90.041801.
- [11] ADAMSON P. *et al.*, *Phys. Rev. Lett.*, **106** (2011) 181801, doi:10.1103/PhysRevLett.106.181801.
- [12] ABE K. *et al.*, *Phys. Rev. D*, **85** (2012) 031103, doi:10.1103/PhysRevD.85.031103.
- [13] PONTECORVO B., *Sov. Phys. JETP*, **26** (1968) 984.
- [14] MAKI Z., NAKAGAWA M. and SAKATA S., *Prog. Theor. Phys.*, **28** (1962) 870, doi:10.1143/PTP.28.870.
- [15] ABE K. *et al.*, *Phys. Rev. Lett.*, **107** (2011) 041801, doi:10.1103/PhysRevLett.107.041801.
- [16] ADAMSON P. *et al.*, *Phys. Rev. Lett.*, **107** (2011) 181802, doi:10.1103/PhysRevLett.107.181802.
- [17] ABE Y. *et al.*, *Phys. Rev. Lett.*, **108** (2012) 131801, doi:10.1103/PhysRevLett.108.131801.
- [18] AN F. P. *et al.*, *Phys. Rev. Lett.*, **108** (2012) 171803, doi:10.1103/PhysRevLett.108.171803.
- [19] AHN J. K. *et al.*, *Phys. Rev. Lett.*, **108** (2012) 191802, doi:10.1103/PhysRevLett.108.191802.
- [20] MARLEAU G. *et al.*, Report IGE-157 (1994).
- [21] MURE (2009) <http://www.nea.fr/tools/abstract/detail/nea-1845>.
- [22] MUELLER TH. *et al.*, *Phys. Rev. C*, **83** (2011) 054615, doi:10.1103/PhysRevC.83.054615.
- [23] HUBER P., *Phys. Rev. C*, **84** (2011) 024617, doi:10.1103/PhysRevC.84.024617.
- [24] VOGEL P. and BEACOM J. F., *Phys. Rev. D*, **60** (1999) 053003, doi:10.1103/PhysRevD.60.053003.
- [25] DECLAIS Y. *et al.*, *Phys. Lett. B*, **338** (1994) 383, doi:10.1016/0370-2693(94)91394-3.
- [26] MENTION G. *et al.*, *Phys. Rev. D*, **83** (2011) 073006, doi:10.1103/PhysRevD.83.073006.